Heterogeneous & Homogeneous & Bio- & Nano-

CHEMCATCHEM

CATALYSIS

Accepted Article

Title: Heterostructured manganese catalysts for the selective oxidation of 5-hydroxymethylfurfural to 2, 5-diformylfuran

Authors: Priyanka Pal and Saravanamurugan Shunmugavel

To be cited as: *ChemCatChem* 10.1002/cctc.202000086

Link to VoR: http://dx.doi.org/10.1002/cctc.202000086

A Journal of ChemPubSoc Europe

WILEY-VCH

www.chemcatchem.org

Heterostructured manganese catalysts for the selective oxidation of 5-hydroxymethylfurfural to 2, 5-diformylfuran

Priyanka Pal and Shunmugavel Saravanamurugan*

Abstract: A series of manganese oxide catalysts were synthesised in the presence of various precipitants using hydrothermal approach. The manganese oxide synthesised (MnOx-A-U) using manganese acetate tetrahydrate and urea as precursor and precipitant, respectively, was found to be composed of heterostructures of manganese, that is, $MnCO_3$, ε-MnO_2 and Mn_2O_3, and their presence were confirmed by XRD, FTIR and XPS analyses. The catalytic activity of MnOx-A-U towards selective oxidation of HMF to DFF in ethanol afforded 92.0% conversion along with 88.0% DFF yield at 120 °C, 30 bar O_2, after 4 h of reaction time. Performing HMF oxidation under N_2 atmosphere with MnOx-A-U yielded only 15.0% DFF, revealing that lattice oxygen played a crucial role in the oxidation process, which was confirmed by subjecting the spent catalyst to XPS analysis. Based on the results obtained from XPS analysis, it was speculated that ε-MnO_2 and $MnCO_3$ could be the active species which could selectively catalyse the reaction. The MnOx-A-U catalyst was able to recycle for at least three runs with a small loss of activity due to ε-MnO_2 content decreased.

1. Introduction

The increasing demand for energy, fuels, and chemicals-derived predominantly from fossil-based resources - has been due to the not only overgrowing population but also increase in the standard of living, especially in the developing countries. However, fossil resources are confined and available for a limited period only, and thus, they cannot meet the future requirement of our society in terms of energy, fuels and chemicals [1-3]. It is highly possible to replace these limited fossil resources with renewable, sustainable feedstock such as terrestrial biomass to keep the value chain. First generation biomass refers to vegetable oil and starch, which are produced from edible sources associated with the food chain. While the second generation biomass refers to lignocellulose produced as waste from, for example, wood, which is abundantly available as a source of carbon and can be utilized to derive chemicals and fuels, as considered to be a carbon-neutral process; thus reducing carbon footprint. In connection with this, a broad range of potential chemicals produced from biomass-derived molecules such as glucose has been widely reported [4-8]. With regard to this, 5-hydroxymethylfurfural (HMF), can be derived from cellulosic part of lignocellulosic biomass via glucose dehydration, has been emerged as a potential platform chemical for producing a broad spectrum of high-value chemicals such as 2,5-diformylfuran (DFF), maleic acid, and 2,5-furandicarboxylic acid (FDCA) [9-11]. Of which, DFF is a partially oxidised product of HMF, having potential applications in pharmaceuticals, fungicides ,furan-urea resins and heterocyclic ligands [12-14] as shown in Fig. 1.

In 2014, Grasselli proposed the concept of “seven pillars” for partial oxidation reactions entailing a redox mechanism. The seven pillars are based on lattice oxygen, metal-oxygen bond, the structure of the host material, redox property, multifunctional character of the material, site isolation and the phase cooperation. Among which, site isolation and phase cooperation are essential and useful to design a suitable material for the oxidation reaction [15]. Related to this, various precious and non-precious metals have been employed for the selective oxidation of HMF to DFF under different reaction conditions either with homogeneous or heterogeneous catalysts [16], as the selective oxidation of HMF to DFF is relatively a challenging process as HMF consists of two reactive functional groups, that is, a hydroxyl group and an aldehyde group, and both tend to get oxidised in the presence of oxygen.

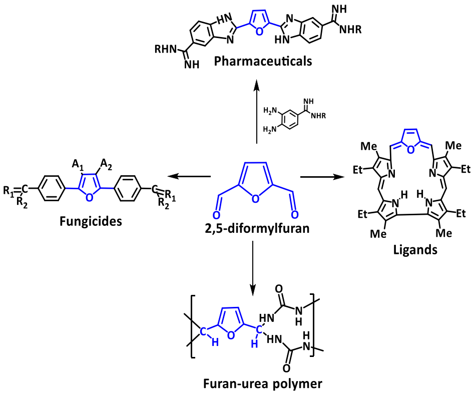

Figure 1. The uses of DFF in various applications [12-14].

In the previous study, the catalysts consisted of $Co^{2+}/Mn^{2+}/Br^{-}$ were used for the oxidation of HMF (82.0%) into DFF (73.0%) in acetic acid at 75 °C under 70 bar air [17]. This process entailed a tedious workup after the reaction for isolating the product from the homogeneous reaction mixture; thus less promising compared to the heterogeneous catalyst system, even though a high yield of DFF was achieved. Various precious metal oxides of Pt, Pd, Ru and Au on supported materials offered a high yield of DFF from HMF under aerobic oxidation conditions [18-23]. For example, Ru/ γ-Al_2O_3 afforded a near-quantitative yield of DFF (97.3%) in toluene at 130 °C, 2.7 bar O_2 [21]. Due to the

---

P. Pal and S. Saravanamurugan
Laboratory of Bioproduct Chemistry
Center of Innovative and Applied Bioprocessing (CIAB)
Sector-81 (Knowledge City), Mohali-140 306, Punjab, India.
*Email: saravana@ciab.res.

Supporting information for this article is given via a link at the end of the document.((Please delete this text if not appropriate)) high cost of the material and solvent and poor stability of the material, alternative non-precious metal(s)-containing catalysts were being considered for replacing the precious metals without compromising the yield of DFF.

Manganese-based materials have been widely used recently due to their variable oxidation states and have a wide application in catalysis, lithium-ion batteries, and supercapacitors [24]. The various manganese-based catalysts in connection with the selective oxidation of HMF to DFF have been employed, and the results are presented in Table S1. Nie and Liu reported that manganese oxide octahedral molecular sieve (OMS-2) yielded 97.0% of DFF at the quantitative conversion of HMF in dimethylformamide (DMF) at 110 °C, 5 bar oxygen [25]. Under identical reaction conditions, other manganese oxides such as Mn_3O_4, Mn_2O_3 and amorphous manganese oxide (AMO) exhibited a lower activity compared to OMS-2. When loading 15 wt% of Ag on OMS-2, the DFF yield of 99.0% was achieved in [26]. Similarly, Mn (III)-Salen catalyst showed excellent activity in terms of DFF yield (89.0%) with a complete conversion of HMF in dichloromethane (DCM) at room temperature [27]. The major challenges in this study were a complex catalyst preparation and very poor recyclability. Interestingly, alterations in the structural morphology of manganese oxide could influence the activity on the yield of DFF. For example, MnO_2 with the morphology of microsphere, blocky type and nanowire type rendered 8.0 and 11.0% and 40.6% of DFF in DMF and MeOH, respectively [28, 30]. When incorporating Au on MnO_2 (microsphere) and Cu on MnO_2 (nanowire type), the yield of DFF increased to 82.0 in DMF and 64.8% in ethanol, respectively [28, 30]. Likewise, Fe_3O_4/Mn_3O_4 and $MnCO_3$ yielded 82.1 and 87.0% of DFF yield with 100% conversion of HMF [31, 34].

The aforementioned catalyst systems entailed a complex synthesis procedure, leaching of metal(s) from the support, toxic and high boiling solvents which are difficult to remove during the separation stage and a high catalytic amount. The pioneer works related to selective oxidation of HMF to DFF prompted us to design manganese oxide catalysts without any auxiliary metal for the same transformation in an environmentally benign solvent. Here we report the preparation of various manganese oxide from acetate and nitrate precursors with various precipitants by precipitation and hydrothermal approaches. The synthesized catalysts were characterized by various techniques to study their physicochemical properties and applied for the HMF oxidation reaction in ethanol. The various reaction parameters were optimized for enhancing the yield of DFF in ethanol. Interestingly, we found that the catalyst (MnOx-A-U) composed of $MnCO_3$, ε-MnO_2 and Mn_2O_3, confirmed by XRD and XPS analyses, showed a highest catalytic activity, yielding 88.0% DFF at 120 °C, 30 bar O_2 after 4 h. To the best of our knowledge, mixed valent heterostructures of manganese (MnOx-A-U) has not been yet reported for the selective oxidation HMF to DFF in ethanol.

2. Results and Discussion

2.1 HMF oxidation with mono- and bimetal oxides

Initially, the oxidation of HMF experiments were performed with various non-precious mono- and binary metal oxide catalysts, prepared by precipitation method using sodium bicarbonate as precipitant, in ethanol at 120 °C, 15 bar O_2, for 4 h, and the obtained results are summarised in Table S2. Among the monometal oxides employed, MnOx, prepared by using manganese acetate tetrahydrate as a precursor, showed a highest DFF selectivity (86.3%) along with 73.0% conversion of HMF (entry 1, Table S2). Other monometal oxides (FeOx, CoOx, NiOx, CuOx and ZnOx) afforded a very poor yield of DFF around 2.2-9.6% with a lower DFF selectivity (16.9-48.0%). As MnOx exhibited a highest catalytic activity and to improve the yield of DFF, binary metal oxide catalysts were also prepared in a combination of MnOx and FeOx or CoOx or NiOx or CuOx with 1:1 ratio and tested them for the HMF oxidation under similar reaction conditions. MnOx-FeOx showed the highest conversion of HMF (91.0%), but the DFF selectivity lowered to 68.4% compared to MnOx (86.0% DFF selectivity), suggesting that FeOx decreased the activity in terms of DFF yield. Other binary metal oxide catalysts showed lower activity in terms of DFF yield (entry 9-11, Table S2) compared to MnOx-FeOx (entry 8, table S2).

2.2 HMF oxidation with MnOx

In order to improve the yield of DFF from HMF with monometal oxides catalyst, manganese oxide was also prepared by hydrothermal treatment using various precipitants such as $NaHCO_3$, NaOH, ammonium carbamate, ammonium hydroxide and urea. The prepared catalysts were employed for HMF oxidation to DFF in ethanol at 120 °C, 15 bar O_2 for 4 h, and the results are presented in Table 1. Under identical reaction conditions, MnOx-U and MnOx-A-U, prepared by using manganese nitrate hydrate and manganese acetate tetrahydrate, yielded 75.6 and 76.7% DFF at a conversion of 78.3 and 81.1% HMF, respectively, with a selectivity of above 94.0 % (entry 5 and 6, table 1). Manganese oxide catalysts prepared with other bases gave a relatively lower yield of DFF between 40.9 and 67.4%. To understand the role of precipitants on the yield of DFF, all the manganese oxide catalysts were subjected to XRD analysis, and the corresponding patterns are shown in Fig. S1. XRD patterns of MnOx-SB, MnOx-SH and MnOx-AC showed that manganese oxide possessed amorphous structure. However, on the other hand, MnOX-AH and MnOx-A-U showed a somewhat sharp crystalline peak (Fig. S1 and Fig. 2). Moreover, MnOx-A-U exhibited peaks at 2θ of 31.5, 32.9 and 37.31 (shoulder peak) which could be ascribed to $MnCO_3$, Mn_2O_3 and ε-MnO_2, respectively, inferring the concerted role of heterostructured manganese (MnOx-A-U) on enhancing the yield of DFF. The characteristic peak of $MnCO_3$ was absent in the cases of MnOx-SB and MnOx-SH as there was no source for carbonate species in the employed precipitants.

Table 1. The influence of various manganese oxide catalysts on the yield of DFF.

Entry	Catalyst	HMF Conversion (%)	DFF Yield (%)	DFF Selectivity (%)
1	MnOx-SB	56.8	53.9	94.9
2	MnOx-SH	40.9	35.5	86.8
3	MnOx-AC	62.0	54.4	87.7
4	MnOx-AH	67.4	65.9	97.8
5	MnOx-U	78.3	75.6	96.6
6	MnOx-A-U	81.1	76.7	94.6

Reaction conditions: 1 mmol HMF, 20 ml ethanol, 100 mg catalyst, 120 °C, 4 h, 15 bar O_2.

To substantiate further the presence of $MnCO_3$ in MnOx-A-U, the as-synthesised MnOx-A-U (before calcination) was subjected to XRD analysis, and the results are presented in Fig. 2. The XRD pattern of MnOx-A-U before calcination was found to be virtually composed of $MnCO_3$, suggesting that the precipitant urea reacted with the precursor manganese acetate tetrahydrate during hydrothermal treatment to form $MnCO_3$ complex which has not been completely decomposed even after calcination at 450 °C for 4 h. The peaks appeared at 24.3° (012), 31.4° (104), 37.5° (110), 41.6° (113), 45.3° (202), 49.7° (024), 51.8° (018), 59.2° (211), 60.2° (122), 63.9° (214), 67.7° (300) for MnOx-A-U before calcination matched well with standard XRD pattern of rhombohedral $MnCO_3$ (space group R-3c, ICSD:080867). On the other hand, in the case of MnOx-A-U after calcination exhibited the appearance of three new peaks along with the characteristic peaks of $MnCO_3$. The new peaks appeared at 32.9° (222), 49.3° (134), 55.3° (440) matched well with the characteristic peaks of bixbyite Mn_2O_3 (cubic, Ia-3) [43]. Moreover, the other peaks corresponding to ε-MnO_2 could also be seen at 2θ of 37.3° (100) and 55.3° (102) [33 (b-c)].

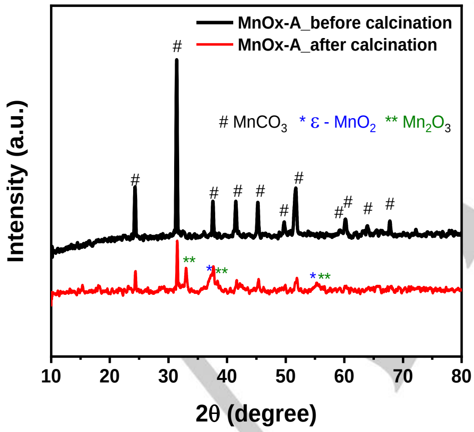

Figure 2. XRD patterns of MnOx-A-U before and after calcination.

The above-mentioned characteristic results revealed that MnOx-A-U is composed of heterostructures of manganese, that is, $MnCO_3$, Mn_2O_3 and ε-MnO_2, which could be responsible for enhancing the yield of DFF compared to other catalysts employed in this study. The presence of $MnCO_3$ on MnOx-A-U was also confirmed by FTIR analysis. Fig. 3 shows FTIR spectra of MnOx-A-U before and after calcination, and displays the presence of characteristic peaks of asymmetric and symmetric vibrational bands of carbonate at 1400 and 850 and 718 cm^{-1}, respectively [45] with high intensity, confirming the presence of $MnCO_3$, as in agreement with XRD analysis. The intensity of the characteristic peaks significantly decreased in the case of MnOx-A-U after calcination, inferring that $MnCO_3$ converted to ε-MnO_2 to Mn_2O_3 during the calcinations. In addition, Mn-O bending vibration could also be seen in the region of 600 to 450 cm^{-1}, as in line with the previously published article [46].

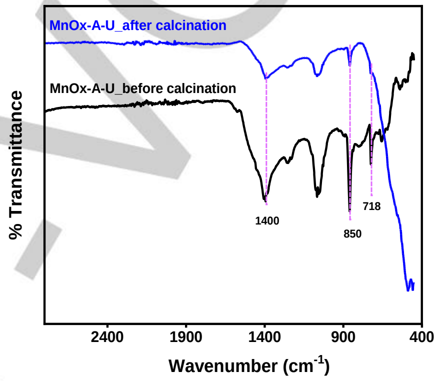

Figure 3. FTIR spectra of MnOx-A-U before and after calcination

To corroborate the role of $MnCO_3$ and ε-MnO_2, MnOx-A-U was treated at high calcination temperature, that is, 600 °C and then tested for HMF oxidation and found that MnOx-A-U-600 lost its activity drastically, giving only 4.9% of DFF (Table S3). However, MnOx-A-U-300 gave slightly higher yield of DFF (56.1%) than MnOx-A-U-450 which could be due to changes in the composition of ε-MnO_2 and $MnCO_3$ and Mn_2O_3 (Fig. S2). The XRD pattern of MnOx-A-U-600 showed that the peak belonged to $MnCO_3$ and ε-MnO_2 almost disappeared, and concomitantly, the peaks corresponding to Mn_2O_3 appeared, manifesting that the absence of $MnCO_3$ and ε-MnO_2 could lead to the significant loss of its activity (Fig. S2). The synthesised MnOx catalysts were also subjected to SEM analysis. Fig. S3 shows no clear morphology for MnOx-SH, MnOx-AC and MnOx-SB, but in the cases of MnOx-A-U and MnOx-AH exhibited a morphology of blocky/cubical and spherical, respectively, having an average particle size of 5-22 and 2 µm.

MnOx-A-U was further subjected to XPS analysis to find out the various oxidation states of Mn. Fig. S4a displays the full survey spectrum of MnOx-A-U, showing peaks for O1s, C1s and Mn2p. The spectrum of O1s showed a major peak at 529.5 eV along with a shoulder peak at 531.0 eV which can be attributed to the lattice oxygen and metal-hydroxyl species, respectively (Fig. S4b) [47]. C1s spectrum exhibited a major peak at 284.6 eV, confirming the presence of carbonate species (288.8 eV) in MnOx-A-U [48]. The Mn2p spectrum showed two peaks, which can be attributed to spin orbit doublet of $Mn2p_{3/2}$ (642.0 eV) and $Mn2p_{1/2}$ (653.7 eV), respectively (Fig. 4). These two peaks consisted of pairs of peaks after deconvolution, the first pair was at 641.8 and 653.4 eV corresponding to Mn^{2+} the second pair appeared at 643.1 and 654.6 eV ascribed to Mn^{3+} and the third pair was at 644.4 and 657.0 eV assigned to Mn^{4+} [49], indicating the presence of $MnCO_3$, Mn_2O_3 and ε-MnO_2.

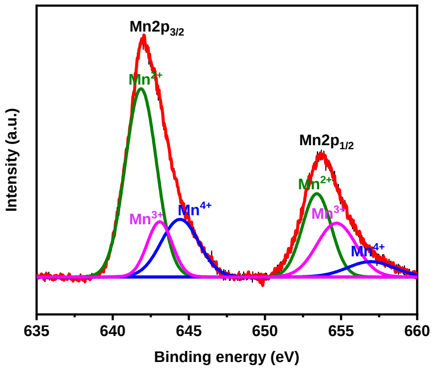

Figure 4. XPS spectra of Mn2p of MnOx-A-U after deconvolution.

2.3 The role of various manganese oxides

As the characteristic results of MnOx-A-U obtained from various techniques revealed the presence of $MnCO_3$ along with Mn_2O_3 and ε-MnO_2, various manganese oxide and $MnCO_3$ were used as catalyst separately under similar reaction conditions to understand their independent role in HMF oxidation. Manganese oxides commercially available (Mn_2O_3, Mn_3O_4 and β-MnO_2) having various oxidation states have been tested for the oxidation of HMF and showed a very poor activity, giving less than 5.0% conversion of HMF with less than 1.0% of DFF yield (Table 2). When employing $MnCO_3$ as catalysts, a very low yield of DFF (<1.0%) was obtained. Under identical reaction conditions, MnOx-A-U composed of $MnCO_3$, ε-MnO_2 and Mn_2O_3 gave fair DFF yield (51.5%) with 98.8% selectivity, signifying the collective role of $MnCO_3$, ε-MnO_2 and Mn_2O_3 on the yield of DFF. It has been previously reported that both tetragonal crystal structure of β-MnO_2 and ε-MnO_2 were active for the conversion of HMF to FDCA, but β-MnO_2 yielded 35% lower FDCA than ε-MnO_2 (60% FDCA) [33b]. Similarly, in another study, ε-MnO_2 showed higher catalytic activity than β-MnO_2 for the oxidation of toluene [52]. These studies revealed that the activity of different phases of MnO_2 depended on the reaction conditions. In a nutshell, it has been speculated that ε-MnO_2 present in MnOx-A-U could play an essential role in the transformation of HMF to DFF under the given reaction conditions in the present study.

Table 2. Oxidation of 5-HMF using various manganese oxide

Entry	Catalyst	Conversion (%)	DFF yield (%)
1	Mn_2O_3	3.40	0.15
2	Mn_3O_4	0.17	0.12
3	β-MnO_2	0.75	0.21
4	$MnCO_3$	2.14	0.97
5	MnOx-A-U	52.1	51.5

Reaction conditions: 1 mmol HMF, 100 mg catalyst, 20 ml ethanol, 120 °C, 1 h, 15 bar O_2.

2.4 Influence of other reaction parameters on the yield of DFF

As MnOx-A-U showed slightly higher yield than MnOx-U, the influence of other reaction parameters such as time, temperature, catalysts loading and O_2 pressure were also investigated with MnOx-A-U, and the results are illustrated in Fig. 5. Fig. 5a shows that from shorter to longer reaction time, no other product was formed but DFF, as HMF can also oxidise to form 5-hydroxymethyl furancarboxylic acid (HMFCA), suggesting the selective oxidation of HMF to DFF with MnOx-A-U. As the reaction time increased, the yield of DFF increased steadily up to 4 h, reaching a DFF yield of 73.7 along with > 99.0% selectivity. The maximum yield of DFF (77.9%) with 88.9 % conversion after 24 h. The optimal temperature and catalyst loading were found to be 120 °C and 100 mg, respectively, yielding 76.7% DFF with MnOx-A-U (Fig. 5b and c). However, a trace amount of 5-formylfurancarboxylic acid (FFCA) was observed. At 200 mg catalyst loading, the yield of DFF decreased significantly due to the formation of FFCA increased from trace to 8.0%. Under 5 bar O_2 pressure, the yield of DFF was 52.0% at 62.0% conversion of HMF with MnOx-A-U. As the O_2 pressure increased to 30 bar, the DFF yield increased to a maximum of 88.3% along with 92.2% conversion of HMF (Fig. 5d). Further, increasing O_2 pressure to 40 bar slightly decreased the yield of DFF (76.6%), concurrently, FFCA yield increased to 9.6% from 2.8% bar (not shown in Fig. 5d) with no formation FDCA. One could expect that when the yield of FFCA increasing, FDCA supposed to have formed. According to the previous studies, it was found that the rate of formation of FDCA from FFCA with activated MnO_2 was relatively slow compared to all other intermediate steps, that is, HMF to FFCA [33b]. Related to this, it has been speculated that a very slow rate of reaction could be one of the reasons that no FDCA formed under given reaction conditions in the present study.

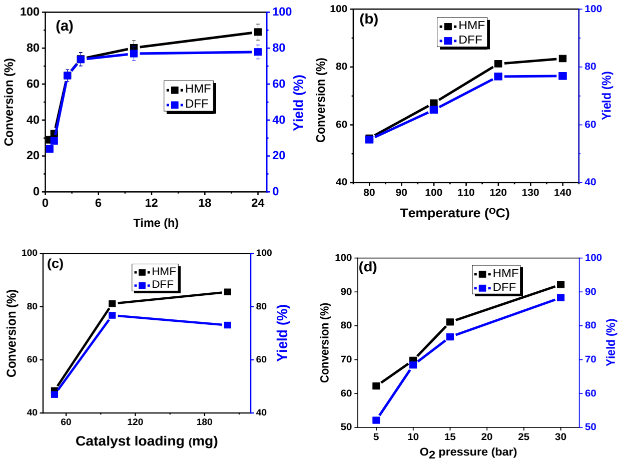

Figure 5. The influence of reaction parameters over MnOx-A-U on the yield of DFF {Reaction conditions: 1 mmol HMF, 20 ml ethanol a) 100 mg MnOx-A-U, 120 °C, 15 bar O_2; b) 100 mg MnOx-A-U, 4 h, 15 bar O_2; c) 120 °C, 15 bar O_2, 4 h; d) 100 mg MnOx-A-U, 4 h, 120 °C}.

2.5 Role of acid and base sites present in MnOx-A-U

It has been reported that acid and base sites could play a role in the transformation of HMF to DFF or FDCA [49]. In line with this, the poisoning of acid and base sites during the reaction was performed independently to probe their role, and the results are summarised in Table S4. When adding an acid additive (2-nitrobenzoic acid), which preferentially passivates basic sites available in MnOx-A-U, during the reaction, only acid sites can contribute to the reaction on the conversion of HMF to DFF, and another way around for adding a base, pyridine. In the case of adding acid additive, 30.1% conversion of HMF along with 28.0% DFF yield was obtained. In the case of adding a base, the conversion of HMF was increased to 46.7%, and the DFF yield increased to 39.8%, displaying that basic sites predominantly participated in the reaction than acidic sites. When using 2-nitrobenzoic acid and pyridine as catalyst separately, the yield of DFF was only less than 1.0%, manifesting no catalytic role of these two additives during the reaction.

2.6 Influence of atmosphere on the yield of DFF

The HMF oxidation reaction was also investigated with MnOx-A-U under various atmosphere, and the results are presented in Fig. 6. Under a N_2 atmosphere, only 15.0% DFF was obtained, indicating that either dehydrogenation or oxidation of HMF by using lattice oxygen. To confirm which pathway this reaction proceeded, the fresh and spent MnOx-A-U in N_2 atmosphere were subjected to XPS analysis and found that the lattice oxygen content decreased from 71.2 to 50.1% (Fig. S5), inferring that lattice oxygen being used for the oxidation of HMF to DFF process, as in agreement with the previous report [25]. Concomitantly, metal-hydroxyl moieties increased from 28.8 to 49.9% (Fig. S5) due to lattice oxygen abstracted the proton from the hydroxyl group of HMF and thus forming metal-hydroxyl moieties [49]. These observations indicated that due to the absence of external oxygen, the redox cycle could not take place, and thus, yielding a low yield of DFF (15.0%). When performing the experiment under air atmosphere, the yield of DFF increased from 15.0 to 46.3% as the amount of available oxygen increased. As external oxygen played a crucial role in participating in the redox cycle by replacing oxygen vacancies, MnOx-A-U yielded the highest yield of DFF (76.7%) under an oxygen atmosphere. Based on these observations and the results obtained from XPS analysis, a plausible reaction mechanism is illustrated in Fig 7.

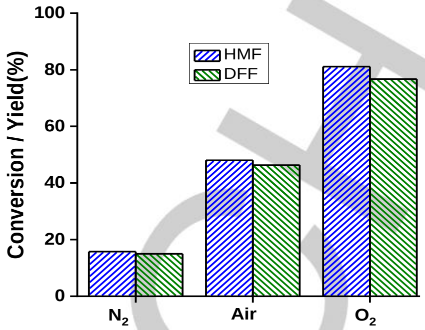

Figure 6. Influence of atmosphere over MnOx-A-U on the yield of DFF (Reaction condition: 1mmol HMF, 20 ml ethanol, 100 mg MnOx-A-U, 120 °C, 4 h, 15 bar).

2.7 Catalytic reaction pathway from HMF to DFF

Initially, Mn (IV) species, possessed more Lewis acidic character, could interact with the oxygen in the hydroxyl group of HMF, and thus, forming metal alkoxide bond along with hydroxyl bond by interacting with lattice oxygen [33]. Concurrently, external oxygen could react with Mn(II)-OH, resulting in the formation of peroxo species (Mn^{3+}-O-O-H), as in line with the reported study [50]. Oxygen vacancy site (O_{vac}) was created as a result of lattice oxygen (O_{lat}) is being used for the formation of a water molecule. Consequently, oxygen in the peroxo species could replace the oxygen vacancy sites, thereby oxidizing the Mn^{2+} to Mn^{4+} and eventually, releasing the DFF; consequently, the redox cycle took place under O_2 atmosphere. Under a N_2 atmosphere, one could expect that Mn(IV) species can catalyze the reaction, but concurrently, due to the absence of external oxygen, the formation of peroxo species prevented due to no external oxygen, and thus, no redox cycle occurred, resulting in a lower yield of DFF (15%).

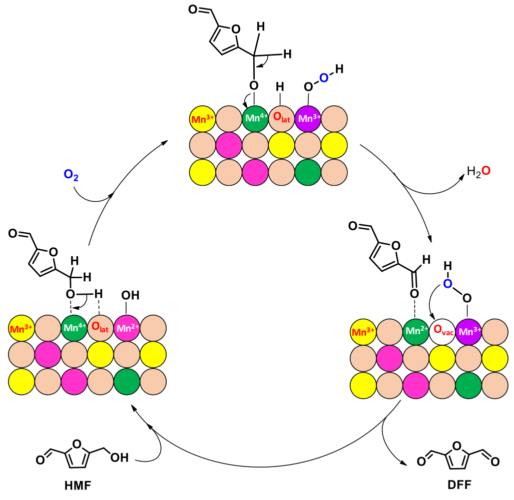

Figure 7. A plausible mechanistic pathway for the transformation of HMF to DFF with MnOx-A-U under O_2 atmosphere.

2.8 Influence of solvent on the yield of DFF

As solvent plays an important role in the oxidation of HMF to DFF, various polar protic, polar aprotic and non-polar solvents have been reported [28-32, 36]. The various solvents, such as water, methanol, acetone, ethyl acetate and toluene were used for the oxidation of HMF with MnOx-A-U, and the results are presented in Fig. 8. Among the solvents employed, MnOx-A-U in water as solvent afforded the lowest yield of DFF (9.6%). Non-polar solvent toluene gave a comparable yield of DFF (29.1%) which was only 3.0% lower than that obtained in ethanol under similar reaction condition, as toluene might facilitate the interaction between the active site in the catalyst and the substrate as proposed in the previous study [36]. For comparison, we have also synthesized two different reported Mn-based materials such as MnOx/P25 and $Mn_{0.5}$+$Co_{0.5}$ [38, 39] according to their procedure and employed as catalysts under the optimised reaction conditions in the present study (Table S 5). $Mn_{0.5}$+$Co_{0.5}$ and MnOx/P25 catalyst systems yielded 30.2 and 5.1% DFF, respectively which was 2.5-15 fold lower catalytic activity than MnOx-A-U in terms of DFF yield, demonstrating that heterostructured manganese played a role on increasing the yield of DFF in ethanol as solvent.

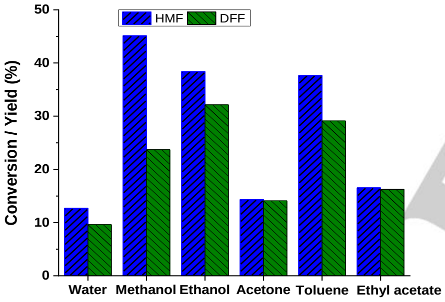

Figure 8. The influence of various solvent with MnOx-A-U on the yield of DFF. (Reaction conditions: 1 mmol HMF, 20 ml solvent, 50 mg catalyst, 15 bar O_2, 120 °C, 1 h).

2.9 Recyclability of MnOx-A-U

Finally, the recyclability of the MnOx-A-U catalyst for HMF conversion to DFF in ethanol was examined at lower conversion at 120 °C for 1 h (Fig. 9). After the first run, 32.4% conversion of HMF along with 87.3% selectivity was obtained. The conversion of HMF slightly increased to 37.5% HMF with 100% selectivity towards DFF. The spent MnOx-A-U after the first run was subjected to XRD analysis (Fig. 10) and found that the intensity of the peak belonging to $MnCO_3$ (31.5°) decreased significantly, concomitantly, the intensity of the peak corresponding to Mn_2O_3 (32.9°) and ε-MnO_2 (37.3°) increased significantly, suggesting that ε-MnO_2 could play a role in enhancing the conversion and selectivity. Moreover, during the calcination, $MnCO_3$ in the recovered MnOx-A-U after the first run could slowly decompose to ε-MnO_2 in the presence of air. However, after the fourth run, the conversion of HMF slightly decreased to 23.0%, maintaining the selectivity of DFF above 98.0%. The XRD pattern of four-time used MnOx-A-U showed a decreased intensity of the shoulder peak corresponding to ε-MnO_2 (37.3°) (Figure 10); thus decreasing the yield of DFF. The XPS spectra of both O1s and Mn2p of the spent MnOx-A-U (after the first use) are shown Fig. S6, and the concentration of Mn^{2+} and Mn^{4+} species along with reactive surface oxygen species (O_{ads}) are also presented in Table S6 [49]. From the Table S6, it can be seen that the amount of Mn^{4+} enhanced by ~4% after the first use, indicating that Mn^{4+} could be responsible for slightly increasing the yield of DFF (Figure 9). Similarly, the reactive surface oxygen species (O_{ads}) increased from 38.5 to 43.5%. It has been proposed in the previous report [49] that O_{ads} species can be transformed into very reactive O_{latt} species which could effectively involve in the redox cycle of Mn^{2+} to Mn^{4+} on the conversion of HMF to DFF as shown in Figure 7. After each run, the spent MnOx-A-U was calcined at 450 °C for 4 h to get rid of any adsorbed organic moieties on the surface of the catalyst. One could expect that during the calcination treatment, $MnCO_3$ could slowly decompose to ε-MnO_2 and then to Mn_2O_3 [51] and consequently, slightly decreasing the DFF yield after the fourth run. It is known that MnO_2 thermally decompose into Mn_2O_3 by releasing O_2 at high temperature (typically > 500 °C). The same phenomenon could be expected to take place when MnOx-A-U repeatedly (three-times consecutively after each run) calcined at 450 °C. The structural changes were also confirmed by FTIR (Fig. S7). The effect of metal leaching, if any, from MnOx-A-U to the solution was also investigated by performing an experiment with MnOx-A-U for an hour at 120 °C, yielding 37.0% conversion of HMF with a DFF yield of 36.0%. After the reaction, the MnOx-A-U catalyst was filtered off, and the homogeneous reaction mixture was further continued for 3 h under similar reaction conditions and found that no significant changes occurred in the conversion of HMF and selectivity of DFF.

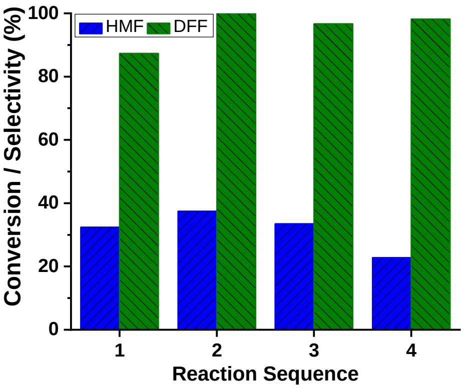

Figure 9. The reuse of MnOx-A-U (Reaction condition: 2 mmol HMF, 20 ml ethanol, 200 mg MnOx-A-U, 120 °C, 1h, 15 bar O_2. After the first run, the scale was adjusted according to the recovered amount of MnOx-A-U to maintain the ratio between the substrate and catalyst and solvent).

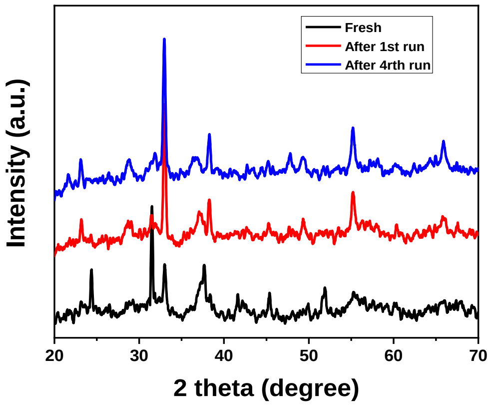

Figure 10. XRD patterns of fresh and spent MnOx-A-U.

3. Conclusions

In conclusion, we have synthesised the heterostructured manganese (MnOx-A-U) catalyst, using manganese acetate tetrahydrate and urea as precursor and precipitant, respectively, which composed of $MnCO_3$, ε-MnO_2 and Mn_2O_3 and applied for the transformation of HMF oxidation in ethanol, yielding a maximum of 88.0% DFF with a selectivity of 95.6%. It was found that MnOx-A-U before calcination exhibited predominantly as a complex of $MnCO_3$, and after calcination, heterostructures of manganese, that is, $MnCO_3$, ε-MnO_2 and Mn_2O_3 formed, as confirmed by XRD, XPS and FTIR analyses. No significant yield of DFF (1.0 %) was obtained when using $MnCO_3$, Mn_2O_3 and β-MnO_2 as catalyst separately. However, the heterostructured manganese (MnOx-A-U) comprised of ε-MnO_2 played a concerted role along with $MnCO_3$ for enhancing the yield of DFF (51.5%) in ethanol under identical reaction conditions. MnOx-A-U calcined at high temperature (600 °C) led to drastically decrease the yield of DFF to less than 5.0%, and the XRD pattern of this catalyst indicated that ε-MnO_2 content significantly decreased, further substantiating the role of ε-MnO_2 for achieving a high yield of DFF. The poisoning study with 2-nitrobenzoic acid or pyridine together with MnOx-A-U revealed that basic sites in MnOx-A-U predominantly participated in the transformation of HMF to DFF. The recyclability study showed that MnOx-A-U could be recycled for at least three times with a small loss of activity due to a decrease in ε-MnO_2 content.

Experimental Section

Chemicals

Manganese acetate tetrahydrate, manganese nitrate hydrate, zinc nitrate hexahydrate, cobalt nitrate hexahydrate, 30% ammonium hydroxide and ammonium carbamate manganese carbonate, manganese dioxide, manganese (III) oxide, manganese (II III) oxide were purchased from Sigma-Aldrich. Copper nitrate trihydrate, ferric nitrate nonahydrate, nickel nitrate hexahydrate and sodium hydroxide were purchased from CDH. Urea and sodium bicarbonate were purchased from TCI.

Catalyst preparation

Various non-precious metal oxide catalysts were synthesized using precipitation and hydrothermal methods by slightly modifying the procedure in the reported literature [42]. In the case of the precipitation method, an appropriate amount of non-precious metal precursor (1.0 to 2.0 g) was dissolved in 5 ml water. To this solution, the aqueous solution of 1 M sodium bicarbonate was added dropwise under stirring until the pH of the mixture reached 9 and allowed for ageing for 4 h. The mixture was then filtered off, washed with plenty of water and ethanol, dried at 80 °C and then finally calcined at 450 °C for 4 h to obtain the corresponding metal oxide catalyst. In the case of hydrothermal method, 3.0 g of manganese nitrate hydrate was dissolved in a minimum amount of water and then added it to the solution containing 50 ml of a 1 M aqueous solution of sodium bicarbonate. The mixture was then allowed to stirring for half an hour. The whole mixture was transferred into a Teflon lined stainless steel autoclave and kept it an oven maintained at 100 °C for 24 h. After cooling down to room temperature, the solution was filtered off, washed with ample amount of water and ethanol, dried at 80 °C, followed by calcination at 450 °C for 4 h to obtain the catalyst (MnOx-SB). The rest of the synthesised manganese oxide catalysts using other bases in place of sodium hydroxide are denoted as MnOx-SH (SH: sodium hydroxide), MnOx-AC (AC: ammonium carbamate), MnOx-AH (AH: ammonium hydroxide) and MnOx-U (U: urea). In the case of MnOx-A-U, manganese acetate tetrahydrate and urea were used as precursor and base, respectively.

Catalyst characterization

X-ray powder diffraction analysis was performed in a PANalytical X'Pert PRO with Cu-Kα radiations (λ = 1.54178 Å) in the range of 10–70° with a scan speed of 2°/min. Lattice parameters and space group were determined by using XpertHighScore software. FTIR spectrum was recorded on an FTIR-ATR spectrophotometer (Spectrum two, PerkinElmer) at room temperature measuring from 450 to 4000 cm^{-1}. Scanning electron microscopy (SEM) images were taken by using a JEOL JCM 6000, Nikon Corporation, Japan) at an acceleration voltage of 10.0 kV. The solid powder was taken on conductive carbon tape and coated with gold in a smart coater (25mm stub size). X-Ray Photoelectron Spectroscopy (XPS) analysis was done by using a PHI 5000 Versa Prob II, FEI Inc. (pass setting of 23.5 eV, 0.025eV Step, 50ms time per step and 10 cycles). Survey scan was done in the range from 0 to 1200 eV with a monochromatic X-ray source of AlKα, and the binding energies were calibrated internally by the C1s binding energy at 284.6 eV.

Reaction procedure

The oxidation of HMF reaction was performed in a high-pressure reactor (Amar, 100 ml vessel) equipped with a mechanical stirrer, a pressure gauge and automatic temperature control apparatus. In a typical experiment, 1 mmol of HMF in 20 ml ethanol and 0.1 g of catalyst were taken in a Teflon cup and then inserted it into the stainless steel vessel. The reactor was then sealed and flushed with O_2 thrice before attaining the required O_2 pressure, and then heated to the desired reaction temperature. After a specific reaction time, the autoclave was cooled down in an ice bath. The aliquot of the reaction mixture was collected by filtering off the catalyst with a 0.22 µm filter prior to the analysis. The reaction mixture was analyzed by high-performance liquid chromatography (Agilent Technologies 1200 infinity series) equipped with RI and UV detector and a HIPLEX-H column at 60 °C. The mobile phase used was 10 mM H_2SO_4 solution at a flow rate of 0.6 mL/min. The conversion of HMF and yield of DFF were calculated based on their individual standards.

Acknowledgements

We gratefully thank the Department of Biotechnology (DBT), New Delhi, India, for support by providing infrastructure facility. SERB-DST is gratefully acknowledged for financial support (ECR/2016/001331), New Delhi, India, and P.Pal is thankful to SERB-DST for a Senior Research Fellowship.

Keywords: manganese oxide• 5- hydroxymethyl furfural • 2, 5-diformyl furan • selective oxidation • heterostructure

References

[1] S. Matar, L. F. Hatch, *Chemistry of Petrochemical Processes*, 2nd Edition, **2001**, *6*.
[2] B. Tian, Y. Qiao, J. Fan, L. Bai, and Y. Tian, *Energ. Fuel.* **2017,** *31*, 10665-10673.
[3] Y. L. Wang, X. H. Chen, M. Ding, and J. Z. Li, *Energ.Fuel.* **2018,** *32*, 796-800.
[4] E. M. Aro, *Ambio*, **2016**, *45*, S24 - S31.
[5] (a) M.S. Holm, S. Saravanamurugan, E. Taarning, *Science*, **2010**, *328*, 602-605; (b) S. Saravanamurugan, M. Paniagua, J.A. Melero, A. Riisager, *J. Am. Chem. Soc.* **2013**, *135*, 5246-5249.
[6] Q. Tang, C. Wua, R. Qiaoa, Y. Chenb, Y. Yang, *Appl. Catal. A: Gen.* **2011**, *403*, 136–141.
[7] A. Corma, S. Iborra, A. Velty, *Chem. Rev.* **2007**, *107*, 2411-2502.
[8] (a) S. Li, W. Deng, S. Wang, P. Wang, D. An, Y. Li, Q. Zhang, Y. Wang, *ChemSusChem.* **2018**, *11*, 1995-2028; (b) P. Ferrini, S. F. Koelewijn, J. V. Aelst, N. Nuttens, B. F. Sels, *ChemSusChem.* **2017**, *10*, 2249-2257.
[9] P. Pal and S. Saravanamurugan, *ChemSusChem.* **2018**, *12*, 145-163.
[10] R. Wojcieszak, F. Santarelli, S. Paul, F. Dumeignil, F. Cavani and R. V. Gonçalves, *Sustain Chem Process*, **2015**, *3*, 9, https://doi.org/10.1186/s40508-015-0034-5.
[11] M. Sajid, X. Zhao and D. Liu, *Green Chem.*, **2018**, *20*, 5427-5453.
[12] (a) K. T. Hopkins, W. D. Wilson, B. C. Bender, D. R. McCurdy, J. E. Hall, R. R. Tidwell, A. Kumar, M. Bajic, and D. W. Boykin, *J. Med.Chem.* **1998,** *41,* 3872-3878; (b) D. W. Boykin, A. Kumar, J. Spychala, M. Zhou, R. J. Lombardy, W. D. Wilson, C. C. Dykstra, S. K. Jones, J. E. Hall, R. R. Tidwell, C. Laughton, C. M. Nunn, and S. Neidles, *J. Med. Chem.* **1995**, *38*, 912-916**;** (c) M. D. Poeta, W. A. Schell, C. C. Dykstra, S. K. Jones, R. R. Tidwell, A. Kumar, D. W. Boykin, and J. R. Perfect, *Antimicrob. Agents Chemother.* **1998**, *10*, 2503–2510.
[13] (a) A. S. Amarasekara, D. Green, L. D. Williams, *Eur. Polym. J.* **2009**, *45*, 595–598; (b) A. Gandini and N. M. Belgacem, *Polym. Int.* **1998**, *47*, 267-276.
[14] M. Ventura, A. Dibenedetto, M. Aresta, *Inorg. Chim. Acta*, **2017**, *470*, 11-21.
[15] R.K. Grasselli, *Catal. Today*. **2014**, *238*, 10–27.
[16] (a) J. Nie, J. Xie, H. Liu, *J. Catal*. **2013**, *301*, 83-91; (b) A. Takagaki, M. Takahashi, S. Nishimura, K. Ebitani, *ACS Catal.* **2011**, *1*, 1562-1565; (c) B. Karimi, H. M. Mirzaei, E. Farhangi, *ChemCatChem*. **2014**, *6*, 758-762; (d) Z. Wei, S. Xiao, M. Chen, M. Lu and Y. Liu, *New J. Chem.*, **2019**, *43*, 7600-7605.
[17] W. Partenheimer, V. V. Grushin, *Adv. Synth. Catal.* 2001, **343**, 102-111.
[18] X. Han, L. Geng, Y. Guo, R Jia, X. Liu, Y. Zhang and Y. Wang, *Green Chem.* **2016**, *18*, 1597-1604.
[19] X. Wan, C. Zhou, J. Chen, W. Deng, Q. Zhang, Y. Yang, and Y. Wang, *ACS Catal.* **2014**, *4*, 2175–2185.
[20] A. Lolli, V. Maslova, D. Bonincontro, F. Basile, S. Ortelli and S. Albonetti, *Molecules,* **2018**, *23*, 2792-2816.
[21] A. Antonyraj, J. Jeong, B. Kim, S. Shin, S. Kim, K.Y. Lee, J. K. Cho, *J. Industrial and Eng. Chem.* **2013**, *19*, 1056-1059.
[22] X. Kong, Y. Zhu, Z. Fang, J. A. Kozinski, I. S. Butler, L. Xu, H. Song and X. Wei, *Green Chem.* **2018**, *20*, 3657-3682.
[23] S. Nishimura and K. Ebitani, *J. JPN Petrol. Inst.* **2017**, *60*, 72-80.
[24] (a) S. L. Suib, *J. Mater. Chem*. **2008**, *18*, 1623–1631; (b) A. J. J. Jebaraj, D. A. Scherson, *Acc. Chem. Res*. **2013**, *46*, 1192–1205; (c) K. Zhang, X. Han, Z. Hu, X. Zhang, Z. Tao, J. Chen, *Chem. Soc. Rev*. **2015**, *44*, 699 –728.
[25] J. Nie, H. Liu, *J. Catal.* **2014**, *316*, 57-66.
[26] G. D. Yadav, R. V. Sharma, *Appl. Catal. B*. **2014**, *147*, 293-301.
[27] S. Amarasekara, D. Green, E. McMillan, *Catal. Comm.* **2008**, *9*, 286–288.
[28] Y. Zhu, M. Shen, Y. Xia, M. Lu, *Catal. Comm*. **2015**, *64*, 37–43.
[29] Y. Zhu and M. Lu, *RSC Adv.* **2015**, *5*, 85579-85585.
[30] X. Tong, L.Yu, H. Chen, X. Zhuang, S. Liao, H. Cui, *Catal. Comm.* **2017**, *90*, 91-94.
[31] B. Liu, Z. Zhang, K. Lv, K. Deng, H. Duan, *Appl. Catal. A.* **2014**, *472*, 64-71.
[32] F. Neatu, N. Petrea, R. Petre, V. Somoghi, M. Florea, V. I. Parvulescu, *Catal. Today*, **2016**, *278*, 66-73.
[33] (a) E. Hayashi, T. Komanoya, K. Kamata, M. Hara, *ChemSusChem*, **2017**, *10,* 654-658; (b) E. Hayashi, Y. Yamaguchi, K. Kamata, N. Tsunoda, Y. Kumagai, F. Oba, and M. Hara, *J. Am. Chem. Soc.* **2019**, *141*, 890−900. (c) F. Shi , F. Wang, H. Dai , J. Dai , J. Deng, Y. Liu , G. Bai, K. Ji, C. T. Au, *Appl. Catal. A: Gen.* 2012, *433*, 206–213.
[34] W. Qi, J. Fang, Z. Yang, B. Li, R. Su, Z. He, *Trans. Tianjin Uni.* **2018**, *24*, 1-7.
[35] S. Biswas, B. Dutta, A. M. Kanakkithodi, R. Clarke, W. Song, R. Ramprasad, S. L. Suib, *Chem. Commun*. **2017**, *53*, 11751-11754.
[36] B. Sarmah, B. Satpati, and R. Srivastava, *ACS Omega*, **2018**, *3*, 7944−7954.
[37] L. Ding, W. Yang, L. Chen, H. Cheng, Z. Qi, *Catal. Today.*, **2018**, 10.1016/j.cattod.2018.04.069.
[38] L. Chen, W. Yang, Z. Gui, S. Saravanamurugan, A. Riisager, W. Cao, Z. Qi, *Catal. Today,* **2019**, *319*, 105-112.
[39] Z. Gui, S. Saravanamurugan, W. Cao, L. Schill, L. Chen, Z. Qi, A. Riisager, *Chemistry Select*, **2017**, *2*, 6632-6639.
[40] ssD. K. Mishra, H. J. Lee, J. Kim, H. S. Lee, J. K. Cho, Y. W. Suh, Y. Yi and Y. J. Kim, *Green Chem.* **2017**, *19***,** 1619-1623.
[41] X. Han, C. Li, X. Liu, Q. Xia and Y. Wang, *Green Chem.* **2017**, *19*, 996-1004.
[42] J. Haber, J. H. Block and B. Delmon, *Pure Appl. Chem.* **1995,** *67*, 1257-1306.

[43] Y. Liu, D. He, H. Wu, J. Duan, Y. Zhang, *Electrochim. Acta.* **2015**, *164*, 154–162.

[44] H. Chen, Z. Yan, X. Y. Liu, X. L. Guo, Y. X. Zhang, Z. H. Liu, *J. Power Sources*, **2017**, *353*, 202-209.

[45] S. Ashoka , P. Chithaiah , C. N. Tharamani and G. T. Chandrappa, *J. Exp. Nanosci.* **2010**, *5*, 285–293.

[46] S. J. Parikh and J. Chorover, *Geomicrobiol. J.* **2005**, *22*, 207–218.

[47] K. Villa, J. Parmar, D. Vilela and S. S´anchez, *RSC Adv*. **2018**, *8*, 5840.

[48] R. Zhang, D. Wang, L. C. Qin, G. Wen, H. Pan, Y. Zhang, N. Tiana, Y. Zhoua and X. Huang, *J. Mater. Chem. A*, **2017**, *5*, 17001-17011.

[49] T. Gao, Y. Yin, G. Zhu, Q. Cao, W. Fang, *Catal. Today.* **2019**, https://doi.org/10.1016/j.cattod.2019.03.065.

[50] J. K. Mobley and M. Crocker, *RSC Adv.* **2015**, *5*, 65780-65797.

[51] F. A. Syed, *Mat. Res.* **2017**, *7*, 79-92.

Entry for the Table of Contents

Layout 2:

FULL PAPER

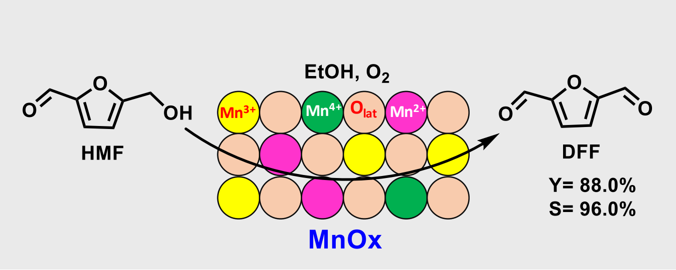

*Priyanka Pal and Shunmugavel Saravanamurugan**

Page No. – Page No.

Heterostructured manganese catalysts for the selective oxidation of 5-hydroxymethylfurfural to 2, 5-diformylfuran

Heterostructured manganese oxide composed of $MnCO_3$, ε-MnO_2 and Mn_2O_3 is employed as catalysts for the selective oxidation of 5-hydroxymethyl furfural to 2,5 diformyl furan, affording excellent yield with near quantitative selectivity.